



# Forecasting the impact of an 1859-caliber superstorm on geosynchronous Earth-orbiting satellites: Transponder resources

Sten F. Odenwald<sup>1,2</sup> and James L. Green<sup>2</sup>

Received 22 June 2006; revised 16 February 2007; accepted 17 February 2007; published 12 June 2007.

[1] We calculate the economic impact on the existing geosynchronous Earth-orbiting satellite population of an 1859-caliber superstorm event were it to occur between 2008 and 2018 during the next solar activity cycle. From a detailed model for transponder capacity and leasing, we have investigated the total revenue loss over the entire solar cycle, as a function of superstorm onset year and intensity.

Our Monte Carlo simulations of 1000 possible superstorms, of varying intensity and onset year, suggest that the minimum revenue loss could be of the order of \$30 billion. The losses would be larger than this if more than 20 satellites are disabled, if future launch rates do not keep up with the expected rate of retirements, or if the number of spare transponders falls below  $\sim 30\%$ . Consequently, revenue losses can be significantly reduced below \$30 billion if the current satellite population undergoes net growth beyond 300 units during Solar Cycle 24 and a larger margin of unused transponders is maintained.

**Citation:** Odenwald, S. F., and J. L. Green (2007), Forecasting the impact of an 1859-caliber superstorm on geosynchronous Earth-orbiting satellites: Transponder resources, *Space Weather*, 5, S06002, doi:10.1029/2006SW000262.

## 1. Introduction

[2] The study of space weather superstorms has increased over the last few years. Although they are historically rare, their ability to affect many important aspects of our current technological infrastructure makes them more than a passing scientific curiosity. For instance, significant concerns are often raised for similarly rare recurrences of the 1906 San Francisco earthquake and exceptional meteorological events. Our understanding of how our infrastructure will behave during severe space weather events is moderated by the fact that, as seen within the broader context of historical solar activity, the current era is actually uncharacteristic of typical solar activity periods during the last 450 years [e.g., *McCracken et al.*, 2001; *Townsend*, 2003].

[3] The study of the record of historic solar proton events (SPEs) since 1561 by *McCracken et al.* [2001] reveals over 125 such events that have left their traces in the nitrite abundances of polar ice cores from Antarctica, Greenland, and the Arctic region. Also, *McCracken et al.* [2001] identified a one-to-one correlation between the seven largest SPEs recorded between 1938 and 1991 and the impulsive nitrite events. The strongest of these 125 events coincided with the 1859 Carrington-Hodgson storm and white light

flare and produced an equivalent fluence of  $1.88 \times 10^{10}$  particles/cm<sup>2</sup>, with an uncertainty in converting nitrite abundances into radiation fluences of  $\sim 30\%$ . Apparently, the solar activity cycles during the satellite era have been uncharacteristically weak in SPE events and fluences compared to the historical record of these events since the year 1567. The frequency of large events with  $>30$  MeV fluences  $>2 \times 10^9$  particles/cm<sup>2</sup> between 1964–1996 averages one event per sunspot cycle, while six to eight such events occurred for sunspot cycles near the years 1605 and 1893. The integrated fluence of the largest five SPEs between 1830 and 1910 was  $5.49 \times 10^{10}$  particles/cm<sup>2</sup> compared with only  $6.7 \times 10^9$  particles/cm<sup>2</sup> during the years 1910–1985. In particular, the satellite era (1967–1994) ranks sixth lowest in the integrated fluences of the strongest six to eight SPEs. The implication is that during the last 400 years, the Sun is most certainly capable of producing a substantially more active satellite environment than what we have come to accept in recent decades. We note that the most recent prediction of the strength of Solar Cycle 24 shows a 30–50% higher peak than in Cycle 23 [*Dikpati et al.*, 2006], but whether this implies a longer-term shift to more typical activity levels of the past is impossible to ascertain.

[4] Recently, *Odenwald et al.* [2006] developed a series of simple “worst-case” models to assess the economic impacts on our current 936-satellite resource as a conse-

<sup>1</sup>QSS Group, Inc., Lanham, Maryland, USA.

<sup>2</sup>NASA Goddard Space Flight Center, Greenbelt, Maryland, USA.

quence of a superstorm that was three times as intense as the 1859 Carrington-Hodgson storm [Tsurutani *et al.*, 2003; Cliver and Svalgaard, 2005; Green *et al.*, 2006] occurring at the peak of the next solar activity cycle in circa 2012. They determined an upper limit of \$70 billion in losses for all satellite systems (geosynchronous Earth-orbiting (GEO), medium Earth-orbiting (MEO), and low Earth-orbiting (LEO)) based on some elementary assumptions about satellite replacement rates, hardware and launch costs, and revenue generation. More important, the models identified a variety of factors whose improved knowledge would make subsequent modeling efforts more robust.

[5] 1. What happens to the assessment when satellites launched after 2004 are included?

[6] 2. What determines a satellite's commercial life span and whether a satellite will be retired or replaced?

[7] 3. How do space weather factors actually impact the generation of satellite revenue?

[8] This paper will refine our previous analysis on the basis of a reassessment of the answers to the above questions. We will derive improved models for GEO satellite operating transponders by using Monte Carlo simulations that calculate the available transponder capacity as a function of superstorm intensity and onset year through the next solar activity cycle (2007–2018).

[9] Following an introduction to the problem in section 1, we will describe our updates to the survey of extant commercial GEO satellites and how they generate revenue in sections 2 and 3. In section 4 we discuss how satellites are removed as a transponder resource via deactivation, failure, and replacement. In section 5 we discuss the mathematical basis and assumptions behind our modeling of the baseline satellite resource, and in section 6 we calculate a baseline model for 1985–2018. We also compare this baseline model with actual satellite industry forecasts and historical data. In section 7 we add a superstorm during years from 2008 to 2018 and calculate the transponder losses as a function of SPE severity. Finally, in section 8 we briefly discuss an economic estimate of superstorm impacts on satellite transponder revenues based upon our models of transponder population size and leased capacity.

## 2. Satellite Resources

[10] For this analysis, we updated the previous estimate ca 2004 for operating satellites by Odenwald *et al.* [2006]. The improved tally (S. F. Odenwald, Archive of operating and planned GEO satellites for the period 1985–2009, 2005, available at <http://www.solarstorms.org/Sscope.html>) of satellites in operation by the end of 2005 includes 906 working satellites of all types. Of these, 289 are GEO communications satellites, which represent the largest commercial segment of the satellite industry and support a \$97 billion per year satellite industry (Satellite Industries Association, SIA releases satellite industries report, press release, 2004, [http://www.sia.org/news\\_events/pressreleases/PR-2004-Satellite%20Statistics\(6-6-05\).pdf](http://www.sia.org/news_events/pressreleases/PR-2004-Satellite%20Statistics(6-6-05).pdf)). This is sub-

stantially larger than the ~\$16 billion worldwide revenues estimated from GPS systems (L. Wirbel, Global positioning system means more than location, 2004, available at <http://www.eetimes.com/showArticle.jhtml?articleID=47212329>) or the \$3 billion from Earth-imaging systems (R. Martin, Pennies from heaven—Earth-imaging companies—Industry trend or event?, *Industry Standard*, 2001, available at [http://www.findarticles.com/p/articles/mi\\_m0HWW/is\\_29\\_4/ai\\_77498003](http://www.findarticles.com/p/articles/mi_m0HWW/is_29_4/ai_77498003)). The 188 LEO communications satellites are of much less value in this economic accounting and will be ignored in this analysis (D. Veeneman, Decode Systems, Iridium, 2004, available at <http://www.decodeystems.com/iridium.html>).

[11] To account for new satellites in operation after 2005, we also include satellite launches after 2005 described in launch schedule summaries by SatNews.com (Planned launches after 2004, available at <http://www.satnews.com/free/planned.html>) as well as information on individual satellite families provided by Gunter's space page (<http://space.skyrocket.de/>), Encyclopedia Astronautica (Spacecraft alphabetical index, 2005, <http://www.astronautix.com/index.html>, Sat-ND), (2005, <http://sat-index.com/failures/index.html>? <http://sat-index.com/failures/telstar401.html>), SpaceLauncher.com (Market prospects 2003 to 2007, 2005, available at <http://www.orbireport.com/Members/Prospects/>), and LyngSat (<http://www.lyngsat.com/launches/2005.html>, <http://www.lyngsat.com/launches/2006.html>, and <http://www.lyngsat.com/launches/2007.html>). We have identified 51 GEO communications satellites to be launched after 2005 for a total of 340 GEO communication satellite systems. Our satellite archive is available online at <http://www.solarstorms.org/Sscope.html>.

## 3. Satellite Transponders as an Economic Asset

[12] Obtaining the correct economic model for geostationary satellite commerce from the open literature is a daunting challenge, given that the details are among the best-kept secrets in the highly competitive, and consequently secretive, satellite industry. In many ways, ferreting out this information from press releases, Web-based satellite and transponder programming archives, and other published documents is a (sometimes futile) exercise in archeology. Nevertheless, we are hopeful that there are some basic ingredients to such a model that are probably universal and fairly uncontroversial.

[13] Satellite revenue is generated by leasing the services of the satellite transponders to clients, who will pay a rental fee (by the hour, day, week, month, or year) for these services. This fee is complicated to estimate because it depends, for a given satellite and a given transponder, on the kind of leasing package that was agreed upon, the particular geographic market being served by the satellite, and the number of clients that are competing to use a particular transponder, which is generally leased to the highest bidder. Also, not all of the available transponders on a given satellite appear to be advertised on the open market. This means that estimating the current load of a

satellite (e.g., number of currently leased transponders) is problematic.

[14] Our satellite transponder model assumes that a given satellite will continue to increase the number of leased transponders at a fixed rate each year until it reaches the limit set by the maximum number of transponders that can be operated at the satellite's available power level. At first, only the excess capacity of the unleased transponders is reduced. Then, at some point in time, the number of leased transponders equals the number that can be operational at the satellite's current power. Finally, as satellite power continues to decline, this phase involves a steady attrition of operating transponders, so the number of leased transponders equals the declining number that can be supported. Once the number of revenue-generating transponders falls below the threshold needed to support satellite operations (typically about \$3 million/year), the satellite operates at a loss and is soon retired. Anecdotal reports of transponder failures and satellite power losses are few; however, there are two recent examples that shed some light on the power-transponder relationship.

[15] In 2006, the AMC-8 satellite lost three circuits on one of its solar panels, which resulted in a loss of 25% of its power. According to news reports, this resulted in no service interruptions, and the transponders could still operate above the minimum acceptable power margin and broadcast level. The loss of a fourth circuit would cause SES Americom to shut off one of the unused satellite transponders. A fifth circuit loss would force the company to turn off "some" of the leased transponders.

[16] In 2001, Arabsat-3A lost eight transponders out of 20 after the satellite was stated to have lost about half its power, according to a report in Space and Tech (<http://www.spaceandtech.com/digest/flash2001/flash2001-109.shtml>). This failure corresponds to a ~40% loss in total satellite transponders stated at launch (20, including 8 spares) and 66% in terms of operating transponders. This suggests that at a power level of 50% beginning of life (BOL), the transponder capacity is also roughly 50% BOL, which is consistent with a report by P. C. Klanowski (Satellite outages and failures, *Satellite News Digest*, 2007, <http://www.sat-index.com/failures/arabsat3a.html>) that the satellite had lost half of its capacity.

[17] From the above reports, we deduce that a satellite operating at 75% BOL can still function at full capacity but with minor changes. At 70% BOL, a single unused transponder may have to be shut down. At 60% BOL, multiple leased transponders may have to be shut down. Finally, at 50% BOL power, major changes in satellite leasing and operations have to occur, with 50% of the transponders taken out of service.

[18] The effect that a solar storm would have on the operating transponders is that if a satellite fails, customer programming is switched to transponders on other satellites owned by the leasing company, provided that such a

contingency was written into the leasing contract. Without this contingency, a customer has to find an open-market replacement. Luckily, because there is currently an oversupply of GEO transponders, it is easy to find available transponders on other satellites at the same longitude. If a satellite experiences only the loss of a few transponders because of a solar power loss, the customer can usually be switched to another available "back up" transponder on the same satellite. For the current analysis, we only consider economic losses to the satellite owner, not to the leasee and the leasee's subscribers.

#### 4. Replacement, Deactivation, and Failure

[19] Our previous study showed that many GEO satellites launched before 2005 will already be near the limits of their productive lives by the next solar maximum in circa 2012. Satellites launched in 1995, for example, will in most cases reach their 15-year end of life (EOL) in circa 2010. Odenwald *et al.* [2006] included the scenario of satellite replacement after 15 years of service, but that analysis was not based on knowledge of whether there were actual plans in place to replace specific satellites. We have expanded the previous analysis by identifying actual, planned, or proposed GEO satellite replacement launches between 2005 and 2008 on the basis of information appearing in Gunter's space page ([www.space.skyrocket.de](http://www.space.skyrocket.de)), Encyclopedia Astronautica (Spacecraft alphabetical index, 2005, <http://www.astronautix.com/index.html>, Sat-ND), Sat-ND (2005, <http://sat-index.com/failures/index.html>? <http://sat-index.com/failures/telstar401.html>), SpaceLauncher.com (<http://www.orbireport.com/Members/Prospects/>), and LyngSat (<http://www.lyngsat.com/launches/2005.html>, <http://www.lyngsat.com/launches/2006.html>, and <http://www.lyngsat.com/launches/2007.html>). There were 15 satellites in our commercial GEO satellite database at least 11 years old by 2005. According to LyngSat (<http://www.lyngsat.com/launches/2005.html>) and SatCODX (<http://www.satcodx1.com/eng/>), these satellites, which we list in Table 1, continue to generate identifiable revenue through a variety of program offerings.

[20] According to Landis and Westerlund [1992], fuel depletion from station-keeping operations has historically determined the end of life for most GEO satellites; however, by 2005, newer station-keeping approaches have substantially reduced fuel usage. The EOL condition now generally involves the failure of the power system or a catastrophic loss of services due to other subsystem failures. Solar array degradation reduces the amount of power available but does not, in general, cause complete failure of a satellite. As the power decreases below the limit set by the currently leased transponders, leased transponders must be shut off, reducing the revenue from the satellite proportionally. We will consider two sources of power loss: gradual losses due to cosmic rays and sudden losses due to solar proton events.



**Table 1.** Old GEO Satellites Still in Operation by 2006

Satellite	Age 2006	Location	Status
Optus-A3	18	164.0E	12 programs
SBS-6	15	286.0E	27 programs
Telcom-2A	14	3.0E	56 programs
Intelsat-K	13	21.5W	5 programs
Thaicom-1	12	120.0E	6 programs
Astra-1C	12	19.2E	37 programs
Gorizont-43	12	140.0E	operating
Intelsat-701	12	180.0E	107 programs
Superbird-2	12	158.0E	11 Programs
Astra-1D	11	23.5E	1 program
Brasilsat-B1	11	70.0W	136 programs
Galaxy-1R	11	133.0W	119 programs
Intelsat-703	11	57.0E	64 programs
PAS-2	11	169.0E	81 programs
Solidaridad-2	11	113.0W	49 programs

#### 4.1. Solar Power Loss Via Cosmic Rays

[21] The gradual decay of solar panel power over satellite lifetimes has been extensively documented since the beginning of the satellite era [e.g., *Tada et al.*, 1982; *Patel*, 2000] and is primarily caused by galactic cosmic rays (GCRs). For satellites in Earth orbit, other contributions to the decline originate through the interactions of energetic MeV protons, ions, and other trapped particles with solar panel cover glass. The degradation occurs at more or less a steady rate each year, and this effect is usually built into the design of the solar panels. Satellite designers use a variety of statistical models (AP8, AE8, CRRESPRO, etc.) to predict solar panel radiation dosages over the planned lifetime of a satellite. This leads to the inclusion of beginning-of-life (BOL) power margins of  $\sim 15\%$  through oversizing the solar arrays to allow for adequate end-of-life (EOL) power. The prelaunch lifetime estimate for a satellite is usually based on the  $\sim 2\%$  per year decline in satellite operating power due to cosmic rays following the analysis of *Chetty* [1991] and *Crabb* [1994]. Newer-generation GaAs/Ge cells used since 1996 are more resistant to this cumulative damage (World Technology Evaluation Center, Large GEO satellites, 1998, available at [http://www.wtec.org/loyola/satcom2/03\\_02.htm](http://www.wtec.org/loyola/satcom2/03_02.htm)) and show very little power loss over comparable satellite timescales. For the purposes of our modeling, we will assume that these changes result in a cyclical, 1.0–1.5%/year BOL power decline for GCRs at GEO between solar maximum and solar minimum. The peak loss is only slightly lower than the overall (SPE plus GCR) 2% cited by *Brekke* [2004] on the basis of SOHO power data at L1.

#### 4.2. Solar Power Loss Via Solar Proton Events

[22] Solar energetic particle events (SEPs) have been known to reduce satellite lifetimes by as much as 6 years for each major event (International Space Weather Clearinghouse, 2006, [http://data.engin.umich.edu/intl\\_space\\_weather/sramp/storms\\_list\\_89.html](http://data.engin.umich.edu/intl_space_weather/sramp/storms_list_89.html)). According to *Brekke* [2004], SPEs during an 80-month operation period for the

SOHO satellite cumulatively resulted in a  $\sim 6\%$  drop in satellite power, in addition to  $\sim 8\%$  for the general GCR decline during the same period. Similar short-term aging of 2–3 years ( $\sim 4\text{--}6\%$  power loss) was seen on the GOES 7 satellite during the March 1991 SPE [*Allen and Wilkinson*, 1993].

[23] Satellite designers allow for this transient component in lifetime and EOL calculations by using average properties of SPEs during the satellite era and, in particular, by factoring in the “worst-case” event provided by the 4 August 1972 SPE. The actual damage and power reduction produced by an SPE depends on both its fluence and its spectral hardness. From the SOHO data compiled by *Brekke* [2004], the four strongest SPE declines in power were the result of the events in Table 2, based on updated power plots by *Simonin* [2005]. Additional data on the SPE spectra are provided by NOAA (Solar proton events affecting the Earth environment, 2004, available at <http://www.sec.noaa.gov/alerts/SPE.html>). From this data, we will use the SOHO data to convert the fluences of hypothetical superstorm events into a percentage power loss. It is important to note that the Carrington-Hodgson flare of 1859 was the largest SPE event in the past 500 years [*McCracken et al.*, 2001], with the capacity to produce life-threatening radiation dosages for manned missions outside Earth’s magnetosphere [*Stephens et al.*, 2005].

[24] Silicon-based solar panels are more susceptible to energetic particle damage than the new-generation GaAs/Ge cells, which were first used for communications satellites in 1996 (e.g., PAS-5). Most commercial satellites launched after 1996 now use the newer cells, which provide 50% more power per kilogram and have a much higher resistance to damage by energetic particles. Our model incorporates available information on the solar panel type used in each satellite since 1996 and modifies the transponder death rate to take into account the difference between silicon- and GaAs/Ge-based satellite power systems.

#### 5. Modeling the Transponder Satellite Resources

[25] The objective of this effort is to calculate transponder losses produced by superstorms for a range of severi-

**Table 2.** SOHO Documented SPEs and Power Losses<sup>a</sup>

Date	Power Decline, %	Proton Flux >10 MeV, pfu	Fluence >10 MeV
14 Jul 2000	2	24,000	11.5
6 Nov 2001	2	31,700	15.0
9 Nov 2000	1.5	14,800	9.1
25 Sep 2001	1	12,900	7.4
29 Oct 2003	1.7	29,500	$\sim 14.0$

<sup>a</sup>Peak proton fluxes are in units of 1 particle/cm<sup>2</sup>/s/str (pfu). SPE fluences are in units of 10<sup>9</sup> particles/cm<sup>2</sup> and are based on 4 $\pi$  fluxes given by *Reedy* [2002].

**Table 3.** Percentage of Solar Proton Events Versus Solar Cycle Year

Year	10 pfu, %	100 pfu, %	1,000 pfu, %	10,000 pfu, %
1	60	40	0	0
2	20	80	0	0
3	64	20	16	0
4	69	14	14	3
5	63	30	0	7
6	51	29	12	8
7	59	27	14	0
8	54	31	8	8
9	53	27	13	7
10	36	36	27	0

ties and arrival times during the next solar activity cycle. The comparison will be made against a baseline model calculated in which no superstorm occurs. This requires that we create, and verify so far as is possible, the transponder capacity for GEO satellites up to 15 years in the future. We then add to this baseline model a perturbation scaled to various severities of a superstorm, occurring during various years.

[26] Many of the relevant satellite, space weather, and superstorm parameters are, of course, not known with certainty during these years, although their likely ranges can be estimated. For this reason, the model will be Monte Carlo based. Each satellite will be represented by a state vector whose current operating power will be modified in a predictable way following the superstorm depending on the severity of the storm. The state of a satellite at a given time will determine the number of leased transponders in operation at the current power level. The sum of the satellite states, integrated over the ensemble in operation at a particular time, will determine the total transponder population size for the entire ensemble of GEO satellites during a given year. In typical Monte Carlo fashion, many simulations will be run with different realizations of the superstorm intensity, onset year, and baseline GCR and SPE space weather conditions.

[27] The satellite state vector,  $S$ , is defined in terms of a set of variables that are fixed and well defined. These are the initial conditions that define the satellite as a resource, its transponder compliment at BOL, its perceived susceptibility to GCR and SPE power losses, the owner, and its location in GEO. These include (1) the BOL satellite power, (2) the number of BOL K band transponders, (3) the number of BOL C band transponders, (4) the number of K band transponders in use by the current year, (5) the number of C band transponders in use by the current year, (6) the satellite owner (which determines priority of where the client gets moved if a transponder fails and cannot be replaced on the same satellite), and (7) satellite longitude (which determines how close satellites are in order to establish where a client is switched in case of an outage).

[28] There are also model-dependent variables that have to be updated by the model and that affect the calculation

of the current economic revenue for the current year,  $T$ . These are (1) the cumulative radiation/SPE dosage by the end of the year, and (2) the current power level in terms of percentage of BOL power.

[29] Our space weather model produces an estimate of the GCR and SPE fluxes and their impact on the reduction of satellite power each year. The impact of these effects on satellite power and transponder function is calculated for each satellite. The power level is then compared to the operating margin to support the transponders.

### 5.1. Space Weather Model: 2006–2018

[30] We have modeled the current state of the GEO satellite system by using actual SPE and GCR data for 1985–2005 to predict what each satellite's operating power will be by 2006. The gradual power decline due to GCRs is estimated from the historical data from the Climax Neutron Monitoring Station (CNMS), which correlates with GCR variations during the current solar cycle [Wiedenbeck *et al.*, 2005]. We have extrapolated this data to cover sunspot Cycle 24 during the period from 2006 to 2018. We have normalized the CNMS data, which we take to be a proxy for the GCR fluxes at GEO so that at minimum it represents a 1.0% solar power decline, and at maximum it represents a 1.5% decline. The extrapolated data for 2006–2018 is also made to follow the alternating pattern of narrow and broad cycles that is a long-term feature of the GCR cycles by using the CNMS data for sunspot Cycle 22 as a proxy for the upcoming sunspot Cycle 24.

[31] For the post-2006 period, the SPE list from <http://www.sec.noaa.gov/alerts/SPE.html> was “folded” for the three Solar Cycles 21, 22, and 23 which span the data from 1976 to 2005. The fluxes of recent SPEs have been tabulated by NOAA (<http://www.sec.noaa.gov/alerts/SPE.html>) with fluxes ranging from 10 to 43,000 particles/cm<sup>2</sup>/s/str (pfu). In Table 3, the percentage of SPEs in each of four decades (0–99 pfu, 100–999 pfu, 1000–9999 pfu, and 10,000–99,999 pfu) is displayed for each cycle year from 1 to 10, with sunspot maximum occurring in years four to five.

[32] For the post-2006 period, a random number generator is used to pick the total number of SPEs for Solar Cycle 24. The total SPEs in Cycles 21, 22, and 23 were 55, 77, and 90, respectively. These SPE totals show a statistically significant, monotonic increase with time from one solar cycle to the next. Our model includes this increase and assumes  $100 \pm 10$  SPE events for Cycle 24. Using a random number generator, we also distribute these events across the 11-year activity cycle on the basis of the distribution in Figure 1.

[33] From an estimate for the total SPEs in a given year, in the third step, we select the fluxes of the SPEs each year on the basis of the distribution in Figure 1. The result of this calculation will be the  $i$ th realization of an alternative SPE history for the next cycle. The  $i$ th realization generates an array  $SPE(i, j, k)$ , where  $j$  is the year,  $k$  is the SPE index (1 to about 110), and  $SPE$  is the flux of the  $k$ th SPE in the  $j$ th year. Once we specify the GCR and SPE events for a

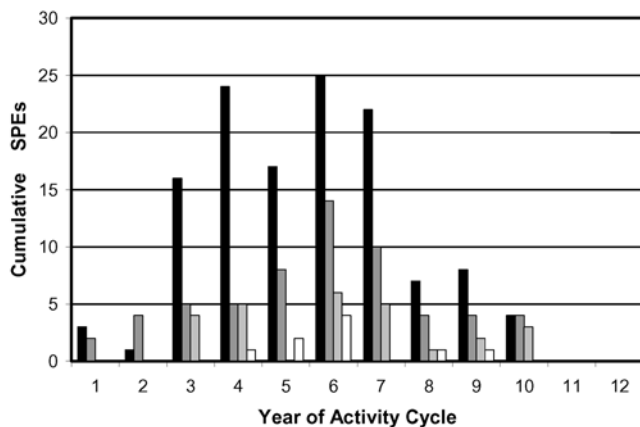


**Figure 1.** Cumulative SPEs for Cycles 21, 22, and 23 for fluxes of 10 pfu (black), 100 pfu (dark gray), 1000 pfu (light gray), and 10,000 pfu (white).

given year, we calculate solar panel power relative to BOL. Each satellite is weighted by its susceptibility to power loss by SPEs and GCRs. For these models, the susceptibility depends on the type of solar panel being used. We assume that GaAs/Ge-based panels are half as susceptible to SPE and GCR damages as silicon-based panels. Since GaAs/Ge-based panels were first utilized in 1996, unless otherwise determined, we assume that satellites launched before 1996 used silicon-based panels, and satellites launched after this year used GaAs/Ge-based panels.

[34] One realization of the baseline space weather conditions for the post-2006 period is shown in Figure 2, in which the dotted line represents the GCR losses and the dashed line represents the SPE losses. Note that the data for the period from 1985 to 2005 are based on actual SPE events and GCR data. We also note that the SPE increase during the period from 2007 to 2018 is consistent with recent estimates that Cycle 24 will be more active than Cycle 23.

[35] In Figure 3, we see the power losses for 100 simulations of the baseline GCR and SPE conditions. Typical GCR conditions yield losses near 1.5% per year, while the SPE conditions vary considerably in frequency and severity. Typical simulations suggest at least one SPE per solar activity cycle, with the capacity to cause 5–8% power losses.

## 5.2. Satellite Launches

[36] Typically, large communications satellites require 18–24 months to construct and launch, so the launch manifest for satellites through circa 2008 is relatively well established by 2006. Most of these satellites are now under construction and have relatively secure launch windows 1–2 years later. The largest uncertainty is in the launch years for currently unannounced replacements for GEO

satellites near the end of their planned service beyond 2009.

[37] Our models were based on the available data, which indicate that after 2008, there are no further planned replacements. Once the satellites launched circa 2000 have reached an average age of 15 years in 2015, the population will necessarily go into decline. Since it is unreasonable to assume that the satellite industry will allow its own satellite resources to go into a decline, we have to assume that a more plausible population distribution will plateau near the current population size circa 2006 of 289 operational satellites and will be maintained at that level through additional launches after 2008.

[38] Forecasting future launch trends is notoriously difficult. Each estimate is based on data that may not be available to all parties. For example, our earlier estimate of 171 commercial satellites to be launched by 2005 or later [Odenwald et al., 2006] was based on publicly available documents. This is different from the prediction of 224 satellites in this population (2005–2014) by Forecast International (Space Daily, U.S. satellite industry dominates despite overcapacity, 2005, available at <http://www.spacedaily.com/news/industry-05zk.html>) based on a more thorough canvassing of industrial sources. *Commercial Space Transportation Advisory Committee (COMSTAC)* [2005, Table 1], meanwhile, forecasted 205 GEO satellites to be launched between 2005 and 2015. Our current, conservative, estimate of 51 launched between 2005 and 2009 is at the lower range of industrial predictions, indicating that we have overlooked a number of satellite systems or that the industrial forecasts include hypothetical systems with little certainty of actual launch. It should be noted, however, that even official forecasts such as COMSTAC [2004] have demonstrated that long-range forecasts (5+ years) can overestimate the number of satellite launches by as much as 50%. This means that their

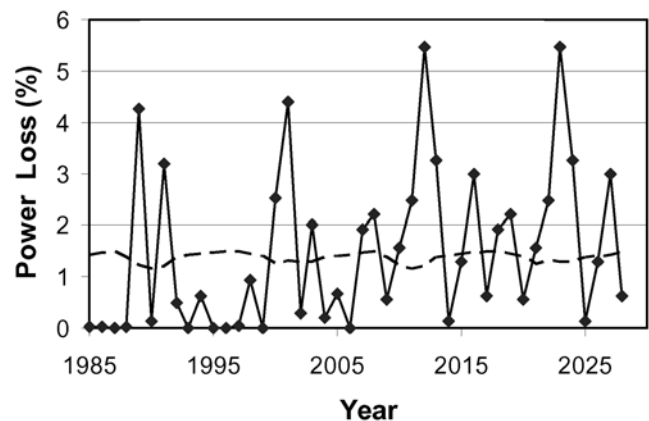


**Figure 2.** Solar panel power loss (%) for GCR (dashed curve) and SPE events (solid curve) for actual conditions (1985–2005) and one simulated forecast (2006–2018).



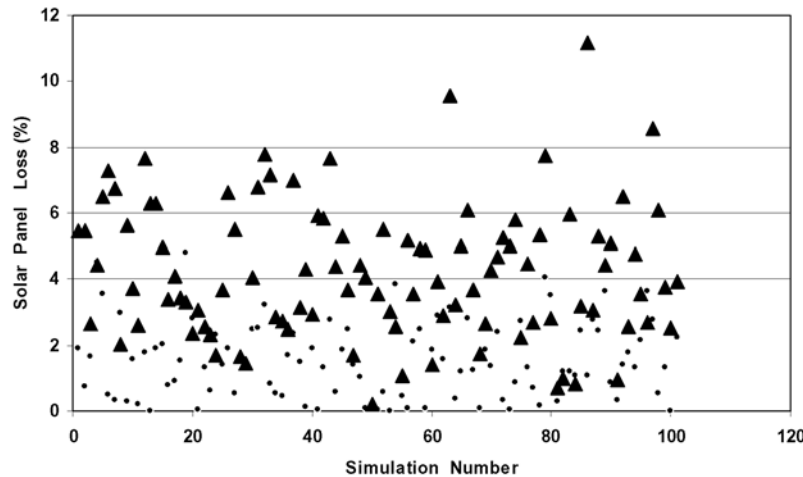


Figure 3. Solar power losses for 100 simulated GCR and SPE baseline activity levels for solar minimum conditions near 2008 (dots) and solar maximum conditions near 2012 (triangles).

estimate could be as low as 100 or as high as 300, making our estimate of 171 within the COMSTAC range of uncertainty.

[39] Our underlying satellite launch and replacement scenario assumes that the satellite industry will replace each satellite that arrives at its planned EOL plus 5 years with a satellite of equal transponder capacity. The newer satellites built after 2006 are assumed to have 15-year life-spans; however, it is not uncommon for modern satellites to survive up to an additional 5 years beyond planned EOL. Between 2005 and 2014, we identify 133 replaceable satellites, including 12 that have already been launched. During this same period, we identify an additional 21 satellites that can be retired. Our estimate of 154 satellites to be retired is perhaps more similar to the COMSTAC estimate of 205 though significantly lower than the 224 suggested by Forecast International. Our ensemble consists of 596 satellites, including 257 hypothetical replacements, and 339 known/operating satellites (288 operational by 2005 and 51 known replacements for 2006–2009). The annual launch rates for the actual (black) and hypothetical satellites (gray) is shown in Figure 4, where we have designated these hypothetical satellites as Hyp-1 through Hyp-257 in the model calculations.

### 5.3. Satellite Response

[40] From the SPE and GCR power losses for the current year, we calculate the current satellite power and the number of transponders that can function at this level. We compare the number of transponders that can be maintained at this power level,  $M$ , with the number that are being leased,  $L$ . If  $M > L$ , no action is taken. The number of leased transponders is increased by the model growth rate for the current year, and the next satellite in the system is selected for updating. However, if  $M < L$ , the model has to

transfer the programming on the unsupported (i.e.,  $L - M$ ) leased transponders to another satellite.

[41] From the host satellite's longitude and the complete list of GEO satellites, we compute the distances to all prospective recipient satellites in the network. We begin with the closest satellite and check to see that it has available transponder capacity. If it does, we check to see that it can accept one additional program without exceeding its own capacity. If it can, we transfer one of the host's programs to the recipient satellite and increase the recipient's leased complement by one. If the recipient satellite cannot accept the program, we look at the next-nearest satellite and perform the same analysis. When the first program has been transferred from the host satellite and there are more programs to transfer, we begin again with the nearest satellite and continue down the list again to find a home for the second program. For example, if

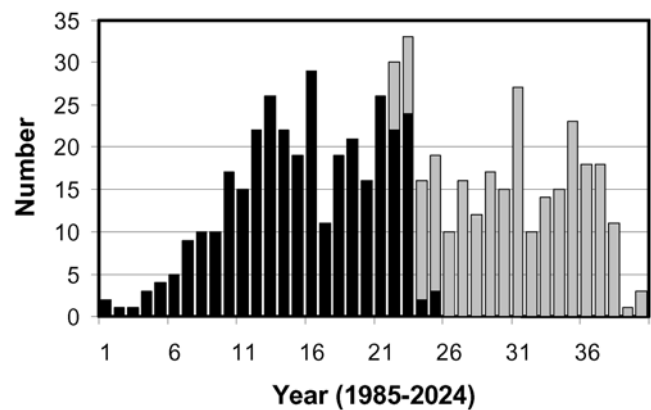


Figure 4. Actual yearly launch history (black) and hypothetical satellite launches (gray) used in our baseline model.

three programs have to be transferred, we perform three cycles of this reassignment process to up to three neighboring satellites. This strategy actually minimizes the risk of losing programs compared to transferring them as a block among satellites that may have little excess transponder capacity to accommodate them.

[42] Once the transfer of the  $L - M$  transponders has occurred, we debit the host satellite so that  $L = M$ . From this point on, the leasing curve,  $L(T)$ , becomes identical to the number of transponders available at the current power,  $M(T)$ , for the satellite. If no satellite backups are available for the programs on the  $L - M$  transponders, the  $L - M$  transponders are permanently lost as a revenue source from the entire GEO network.

[43] Because we identify a program with a transponder and do not model the granularity of programs within a transponder, we use “transponder” and “program” interchangeably because we only use one variable in the mathematical model to represent both concepts. A “lost” transponder means a program that was once carried by a satellite that could not find a home on a neighboring satellite in order to continue providing its content to subscribers. Its original host transponder was deactivated and was lost from service just as the program was also lost from service. A transponder is “lost” because for a given year,  $M$  is less than  $L$ , so  $L - M$  transponders can no longer be supported. Their programs have to be transferred to other satellites. If there are no available transponders on other satellites, these  $L - M$  programs are “lost” from service. In the case of catastrophic damage, all  $L$  transponders are deactivated, and their programming has to be transferred. This is where problems of insufficient capacity elsewhere can occasionally lead to lost programs.

[44] A satellite can only operate on transponder frequencies for which the FCC has issued a license at that orbital location. Generally, a license will not be granted for activation of a transponder if its operation frequency matches that of a transponder on another satellite already operating. The FCC licensing process can take days or weeks, but we assume that at the 1-year resolution of this model, the transfer is fully approved during the year of the loss. In this analysis, we make no distinction between the case where the same company owns both the host and recipient satellites (e.g., Telstar 401 and 401R) and one in which the owners are different companies (e.g., Aramsat-3A and PAS-5). The former case is more restrictive and will only serve to increase the overall lost transponders due to a superstorm. All of these models are, of course, contingent on the assumed rates of transponder leasing growth. Small changes in the growth rates forecasted 10 years into the future will, of course, change the availability of satellites to accept programming from distressed satellites and will thereby alter the calculation of lost transponder programming.

[45] An example of one of our satellite models for a particular realization of the space weather conditions is shown in the timeline in Table 4. Telecom-2A, which

launched in 1991, had a lifespan of 10 years and carried 11 K band and 10 C band transponders. It was replaced in 2001 by AtlanticBird-2, launched in 2001 with a lifespan of 12 years, carrying 26 K band transponders only. In 2018, Atlantic Bird-2 was, in turn, replaced by a hypothetical satellite we designate as Hyp-146. Our model suggests that in 1996, the programming from one K band transponder was transferred to Telecom-2B (colocated with Telecom-2A) because by 1996, the solar panel power loss allowed only 9 operating transponders, which was down from 10 that were available and fully leased during the previous year. A similar situation occurred in 1999, but in this instance, the transponder programming was transferred to Thor 2, located  $7.2^\circ$  from Telecom-2A. The K band programming was assumed to be transferred to Atlantic Bird-2, which only carried K band transponders. The C band programming from Telecom-2A, meanwhile, was transferred to Telecom-2B in 2001.

[46] For Atlantic Bird-2, there were no neighbors within  $15^\circ$  that would have had available capacity to accept transponder programming from this satellite. The candidate satellites were either too old and were already fully leased or had not been launched as yet. As a result, the programming from 10 transponders was lost. Only by 2016 was a hypothetical satellite (Hyp-128) available to handle the programming from two of the Atlantic Bird-2 transponders. Hyp-128 was the hypothetical replacement for Express-A3. This transfer leads to some interesting issues related to commercial transponder access that were not fully covered in the current modeling activity. Although Atlantic Bird-2 is owned by the European company Eutelsat, Express-A3 is owned by Russia. It may not be reasonable to assume that Express-A3 would be available to non-Russian program access in 2016, despite the fact that the satellite industry is becoming more cosmopolitan. In that case, the two K band transponders on Atlantic Bird-2 would be lost from service in 2016. Generally, by allowing these kinds of transactions to take place, regardless of satellite ownership, our models will be underestimating the number of transponders lost from service, making our estimates the lower limit of what is likely to be the actual situation.

## 6. Baseline Model Validation (1985–2018)

[47] The baseline model includes 339 known operational GEO satellites and their planned replacements, along with 257 hypothetical replacements. The models were computed from 1985 to 2006, and the results were compared with industry-wide, publicly available assessments of various parameters to validate the model. We have determined that by 2005, transponder utilization was near 60%. The total number of leased transponders predicted by the model is now within 10% of the *Northern Sky Research* [2005] level of 4150 units. The growth of K band transponders is within 10% of the Futron Corporation’s estimate of ~640 new units between 2000 and 2003 (How many satellites are enough?, 2003, available at <http://www.satelliteonthenet.co.uk/>



**Table 4.** Baseline Simulated Transponder History for Host Satellite Telecom-2A

Year	Power	K Available	C Available	K Leased	C Leased	K Transferred	Recipient Satellite
<i>Telecom-2A</i>							
1991	100	11	10	4	3		
1992	99	10	9	6	5		
1993	97	10	9	8	5		
1994	96	10	9	10	7		
1995	94	10	9	10	7		
1996	92	9	8	9	8	1	Telecom-2B
1997	91	9	8	9	8		
1998	89	9	8	9	8		
1999	87	8	8	8	8	1	Thor-2
2000	86	8	8	8	8		
<i>AtlanticBird-2</i>							
2001	100	26		10			
2002	94	23		16			
2003	93	23		21			
2004	91	22		22			
2005	90	22		22			
2006	89	21		21		1 lost	
2007	88	21		21			
2008	85	20		20		1 lost	
2009	82	19		19		1 lost	
2010	81	18		18		1 lost	
2011	79	18		18			
2012	76	17		17		1 lost	
2013	70	14		14		3 lost	
2014	66	13		13		1 lost	
2015	65	13		13			
2016	63	12		11		2	Hyp-128
2017	59	10		10		1 lost	
<i>Hyp-146</i>							
2018	100	26		10			Hyp-146

white/futron5.html). The growth of C band transponders is also within 10% of Futron's estimate of 260 new units during the same period.

[48] Consistent with the forecasts by Northern Sky Research, we assume a 20% growth in K band and 10% growth in C band transponders during the post-2006 period. Transponder leasing increases at these annual rates until it equals a satellite's available capacity and then declines in step with the transponder capacity dictated by available power until 30% BOL is reached. It is assumed that satellite transponder capacity follows a straight-line curve which is 100% at BOL and 0% at 30% BOL.

## 7. Baseline Plus Superstorm Models

[49] We now add a superstorm to the above baseline model and investigate the transponder population impacts as a function of the storm onset year,  $T$ , and storm strength,  $I$ . To do this, we evaluated the model for 1000 random pairs of  $(T, I)$ . We varied the onset year over the range 2008–2018 and the associated SPE strength over a range from 40,000 to 200,000 pfu. The most intense SPE in our mode was comparable in flux to the 1859 Carrington–

Hodgson superstorm and about four times the strength of the 23 March 1991 SPE (43,000 pfu). As a comparison, the 4 August 1972 SPE corresponded to about 20,000 pfu at its peak for protons >30 MeV [Smart and Shea, 1990].

[50] We have also included the catastrophic loss of up to 20 satellites selected at random from the satellite population for storms in excess of 100,000 pfu. This number of satellites taken out of service is comparable to the total number of damaged satellites during the entire sunspot Cycle 23 (1996–2006). The number of satellites lost is determined randomly within the range [0, 20] for each simulation and among the population of satellites in operation at the time of the storm event. The record of satellite outages during Cycle 23 is only weakly, if at all, correlated with SPE strength (which is our independent variable). For example, Telstar 401 was lost on 13 January 1997, but there was no SPE at that time; meanwhile, no GEO satellites were reported in the open literature as having been “lost” during the major August–October 1989 events with intense SPE activity. When a satellite is lost, its transponder programming is immediately transferred to other available satellites. This is in keeping with most satellite leasing policies which guarantee replacement services to transponder leasees under conditions of

catastrophic loss. This has a beneficial impact on our GEO network. So long as clients have the proper contracts in place with satellite owners to handle these emergencies, it is actually very hard to “lose” transponder programming even during a superstorm. Most satellite owners have contracts that guarantee a replacement satellite will be found for programming that has to be transferred in an emergency, such as when a transponder fails and no backup is available on the satellite. That works in our favor because instead of  $20 \text{ satellites} \times 48 \text{ transponders} = 960$  transponders being lost during a storm, only  $20 \text{ satellites} \times \text{a few transponders} = \text{a few dozen transponders}$  may actually be lost. Our simulations, perhaps fortuitously, reflect this realistic situation.

[51] We calculated the cumulative K and C band transponders lost as a function of storm onset year and strength. The results of these 1000 Monte Carlo simulations are summarized in the two tracks shown in Figures 5 and 6. Interpreting Figures 5 and 6 requires some allowance for the random variations generated by the Monte Carlo simulation itself. We show in Figures 5a and 5b two separate 1000-point simulations. Each uses completely different random number seeds to highlight any statistical variance due to the simulation process itself. There are typically 5000 transponders at play during any given simulation. The random  $N^{1/2}$  error in such a sample is of the order of 70, so we should expect to see non-Gaussian or Poisson behavior for any parameter that is based on approximately a few hundred transponders, which is the case for the “lost” transponders. The artifacts and other features seen in Figures 5a and 5b at this level are simply not statistically significant in our interpretation. About all one can say about Figures 5a and 5b is that the number of lost transponders remains fairly constant to within the statistical variance of  $\pm 70$  and that there is some indication that after our satellite “kill” threshold of 100,000 is reached, the dispersion of the models increases slightly. This is, of course, our previously mentioned ad hoc threshold for killing satellites because of catastrophic events. The dispersion increases because of the particular circumstances of the satellites lost, both in terms of their numbers and the numbers of transponders they contain.

[52] Figure 7 shows that as the severity of the storm increases, the number of program transactions decreases. This seemingly counterintuitive result can be understood once we review why these transactions occur within the model. Transactions will be conducted if (1) the satellite power declines and leased transponder programming has to be moved; (2) a satellite replacement does not have enough BOL capacity to accommodate all of the leased programs on its predecessor; or (3) a satellite has been disabled and its leased transponder programming has to be moved. The severity of a storm can cause rapid changes in conditions 1 and 3; however, old satellites that are catastrophically lost by large storms have fewer programs to transfer if they are disabled (condition 2) or if they experience a large power decrease (condition 1). The

result is that numerically fewer transactions occur during severe storms. Figure 8 also shows that as the storm onset year becomes later, more transactions occur. This is a direct consequence of the overall aging of the satellite fleet and the decrease in the available transponder capacity for each satellite. With fewer unused transponders available in older satellites, more transfers of programming have to occur. This would seem to contradict our initial assumption of a steady state satellite fleet during any given year. For such a steady state fleet, the distribution of ages should be nominally stable, with a mean that is roughly constant over time. This, however, turns out not to be the case. The 1:1 replacement of retired satellites still results in a steady increase in the average age of the “fleet” over the interval of the simulation. This is because, although the typical number of satellites in operation each year is  $268 \pm 8$ , only 6 satellites are replaced in circa 2006, increasing to 18 replacements in 2018. This replacement rate is enough to maintain the satellite population at nearly constant levels but not enough to overcome the aging of the satellite population itself. By 2018, the mean age has increased to about 10 years from an initial 6 years during 2006.

[53] A better metric to use to assess how many transactions are occurring is to normalize the data in Figure 7 to the maximum available capacity of the satellite. In Figure 9 we see that by 2018, the satellites are still operating with  $\sim 35\%$  of their K band transponders leased compared to the number of available BOL transponders. Currently, industry reports suggest that 60% of the available transponders are leased, which means that the industry has about 40% of its BOL transponders as excess capacity or available as backups. During the 2008–2018 period, satellite power levels will decline, allowing fewer of the BOL transponders to be available as spares, so excess capacity will be eroded. The actual working capacity in our simulations is smaller each year than the BOL benchmark because of SPE and GCR solar power declines. When this is factored into our capacity estimates, we see that by the end of the next sunspot cycle, the average satellite is operating with about 50% of its available transponders being leased for the most severe superstorms. We also note that prior to the superstorm onset year, simulated leased capacities were typically from 65% to 80% BOL. Clearly, superstorms do reduce the population of transponders that could be commercially available, but this only serves to reduce large overcapacities already built into most satellite systems and does not cause substantial losses of service.

[54] By combining the data in Figures 8 and 9 into Figure 10, we can normalize the number of transactions occurring at a given superstorm intensity by the number of leased transponders. This essentially gives a per capita activity level for the transponder population and compensates for the declining number of available transponders in the satellite network during later years of the activity cycle. A value near 1.0 for weak storms ( $\sim 40,000$ ) would suggest a

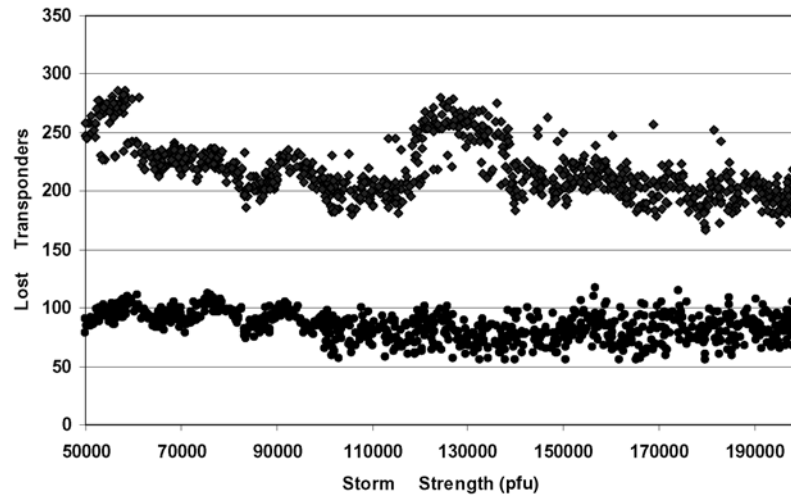


**Figure 5a.** Number of lost K band (diamonds) and C band (circles) transponder programs versus the strength of the superstorm. The vertical dispersion in each group of points follows the increase of the storm onset years from 2008 (lower envelope) to 2016 (upper envelope).

level of activity analogous to what the satellite system experiences during a typical severe solar storm similar to, for example, the Halloween 2003 or the 6 November 2001 storms. The upper envelope of Figure 10 is intuitively straightforward and shows that as the storm strength increases, the number of transactions in the system increases by as much as 30% over the no-storm state. This envelope is defined by storms arriving during the last years of the activity cycle. During these years, there are simultaneously more transactions occurring and fewer numbers of leased transponders in the system; hence the ratio of these factors increases. The lower envelope of Figure 10 is puzzling in that it suggests that when storms arrive early

in the sunspot cycle (circa 2008), transponder activity is essentially independent of storm strength. A possible reason for this is that during the early years of the solar cycle, the satellite system is dominated by younger satellites with plenty of unused capacity. This means that even the most severe storms may not force the transfer of programming but instead merely force satellite owners to use their unused capacity.

[55] The interesting outcome of the current simulations is to reaffirm that the best mitigation strategies for avoiding major financial losses among these satellites are (1) to adhere to a regularly scheduled program of satellite replacements once satellites reach their planned lifetime

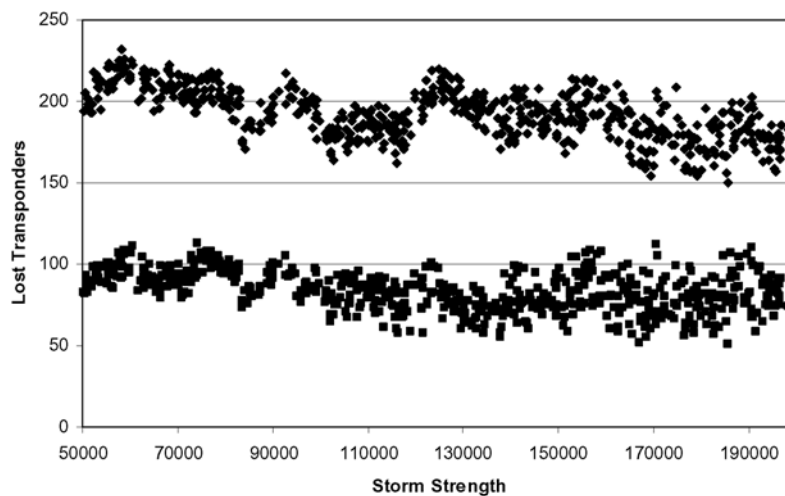


**Figure 5b.** Recalculation of Figure 5a using a different realization of the random numbers in the simulation to evaluate statistical variance.





Figure 6. Total transponders as a function of storm onset year (K band, diamonds; C band, squares). The vertical dispersion is due to the variation of the storm strength from 50,000 pfu (lower envelope) to 200,000 pfu (upper envelope).

limits and (2) to preserve a large margin of backup transponders so that there are plenty of available spares. So long as the number of catastrophically damaged satellites remains below 20 for a superstorm event, it appears that the long-term consequences of their loss is relatively minimal compared to the transponder population size of the surviving satellites.

[56] These simulations consider only SPE effects that erode satellite solar power systems. They do not consider a detailed, self-consistent model of catastrophic damage caused by electrostatic discharges or satellite anomalies that precipitate other subsystem malfunctions. We have

employed an estimate of no more than 20 satellite fatalities for an 1859-caliber superstorm based on a plausible ballpark approximation drawn from the cumulative number of system failures plausibly attributed to space environment effects during the entire 1985–2005 era.

## 8. Some Preliminary Economic Estimates

[57] We can calculate the revenue generated by the transponder population by multiplying the number of leased transponders at any given time by the typical annual lease rate for the service. In our previous analysis

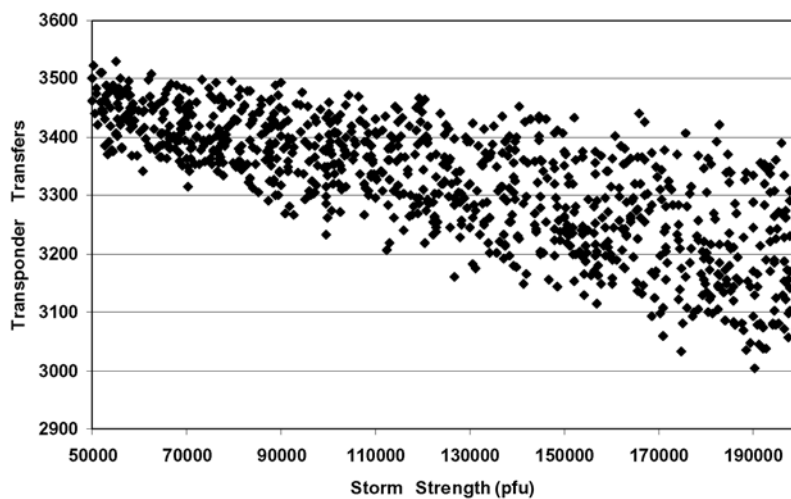


Figure 7. Cumulative number of transfers of transponder programming between satellites. The vertical dispersion is due to the variation of the onset year from 2008 (lower envelope) to 2016 (upper envelope).

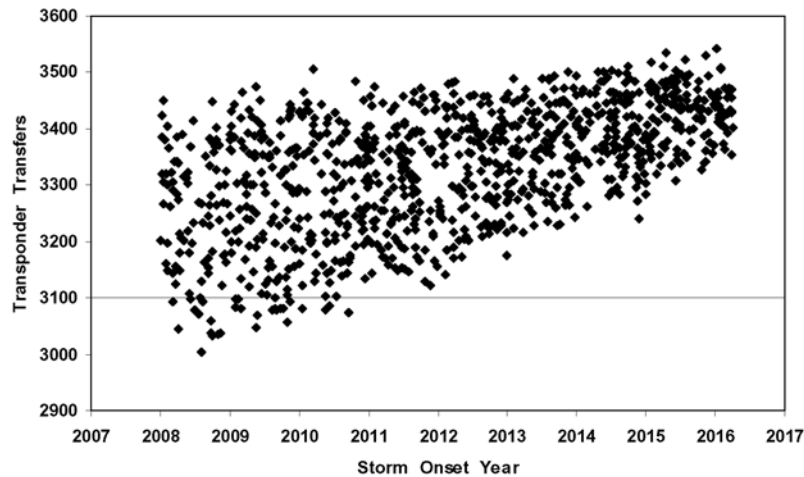


Figure 8. Cumulative number of transfers of transponder programming between satellites. The vertical dispersion is due to the variation of the storm strength from 50,000 pfu (lower envelope) to 200,000 pfu (upper envelope).

[Odenwald *et al.*, 2006], we used an average rate of \$1.5 million per year for each K and C band transponder. These annual rates actually have a significant variation from market to market. In this analysis, we will use the leasing rates for K and C band transponders in six geographic zones. The rates are given in millions of dollars per year in K and C band, i.e., (K, C): North America (2.1, 1.8), South America (2.0, 1.6), Europe (4.0, 0.5), the Mideast (2.0, 1.5), Africa (1.8, 1.4), and Asia (1.8, 1.4) on the basis of the estimates by L. Journez (A recipe to get through the crisis?, 2005, available at <http://www.satelliteonthenet.co.uk/white/vista2.html>). Note that for the highly competitive European market, K band rates have been bid up to \$4.0 million/year, while the less popular C band capacity at \$500,000/year is the least expensive worldwide. Because it is impossible to know how supply and demand will modify these lease rates during 2007–2018, we assume for the time being that the rates remain essentially fixed at the current levels.

[58] By 2018, our baseline, nonstorm model predicts that the cumulative transponder revenue is approximately \$240 billion (in 2006 dollars). As the strength of the superstorm increases, Figure 11 shows that the cumulative revenue by 2018 declines by about \$30 billion over the range of the calculation. This decline makes sense because weaker storms should result in fewer satellites having to lose transponders and therefore more revenue derived from them from stronger storms. Figure 12 also shows that as the onset year increases, the cumulative revenue increases. This occurs because there are progressively more years available for revenue to accumulate as the storm is pushed later and later in the solar activity cycle. Our 1859-caliber superstorm with  $\sim 150,000$  pfu would generate a minimum revenue of about \$210 billion com-

pared to a nonstorm baseline average of \$240 billion, for a net baseline-subtracted revenue loss of approximately \$30 billion.

## 9. Conclusion

[59] We have calculated baseline space weather models for Cycle 24. We have coupled GCRs and SPEs with solar panel degradation and from a detailed model for GEO satellite transponder capacity as a function of superstorm onset year and intensity. From Monte Carlo simulations, we estimate that a 1859-caliber superstorm could result in a loss of approximately \$30 billion in revenue over the course of Cycle 24 (e.g., 2007–2018). This assumes the

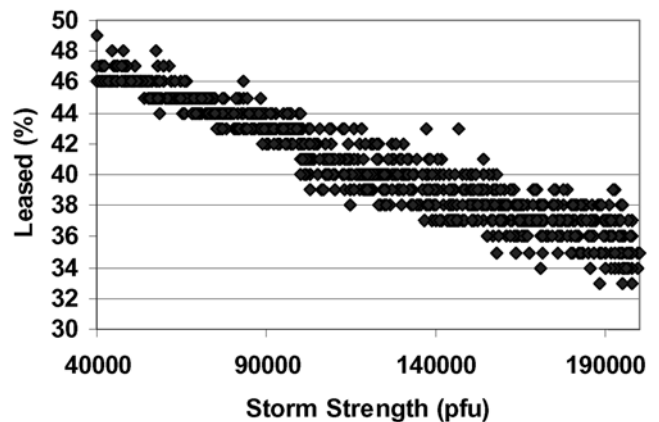
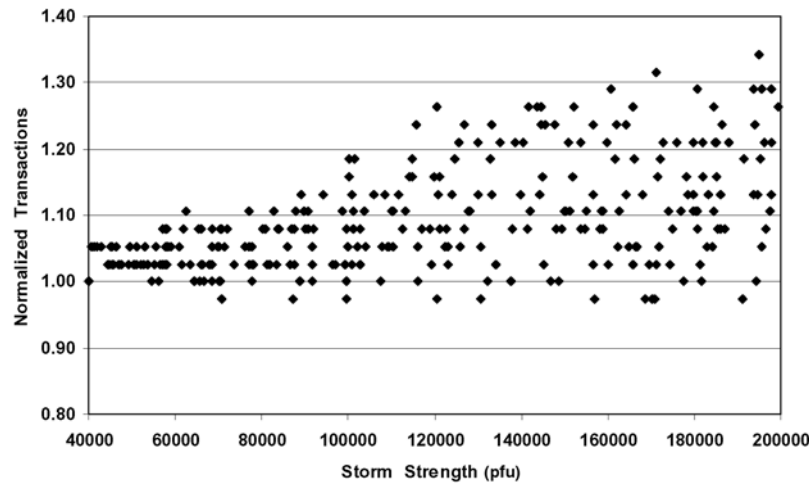


Figure 9. Percentage of leased transponders available by 2018 as a function of superstorm strengths. The decline largely reflects the loss of backup transponders that were not leased.



**Figure 10.** Number of transactions normalized to the number of available transponders each year, as a function of superstorm intensity. The vertical dispersion is due to the variation in the onset year from 2008 (lower envelope) to 2016 (upper envelope).

most favorable satellite replacement strategy in which satellites are regularly replaced when they reach their nominal retirement age, significant transponder utilization margins are maintained, and there is no net growth in the size of the satellite constellation beyond  $\sim 300$  units.

[60] In this simulation, we have not considered certain additional factors in detail, and these may act to increase the economic impact of severe storms and superstorms. The most significant of these are as follows.

[61] 1. Although we attempted to quantify the loss of capacity for each satellite due to GCRs and SPEs, we did not apply a consistent model to predict satellite anomalies that can cause catastrophic satellites losses. *Odenwald et al.*

[2006] estimated that during an 1859-caliber storm, satellite anomalies may be experienced at 100 times the rate of the most severe storm experienced during Cycle 23, with a major escalation in satellite subsystem fatalities. Following a superstorm, many satellites may be operating on backup systems as a consequence of previous storm events, placing them in a precarious situation for the next storm events following the superstorm. If, as for 1859, there are two storms following close together, satellites forced to use backup systems by damage from the first storm may fail when the secondary systems are disrupted by the second storm.

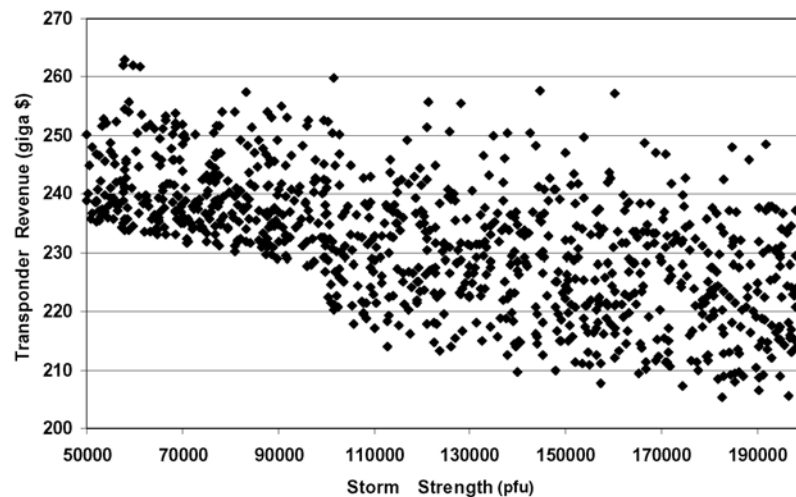


**Figure 11.** Cumulative transponder revenue versus storm strength. The vertical dispersion is due to the variation of the onset year from 2008 (upper envelope) to 2018 (lower envelope). The discontinuity near 100,000 pfu is a result of the threshold level for "killing" satellites.



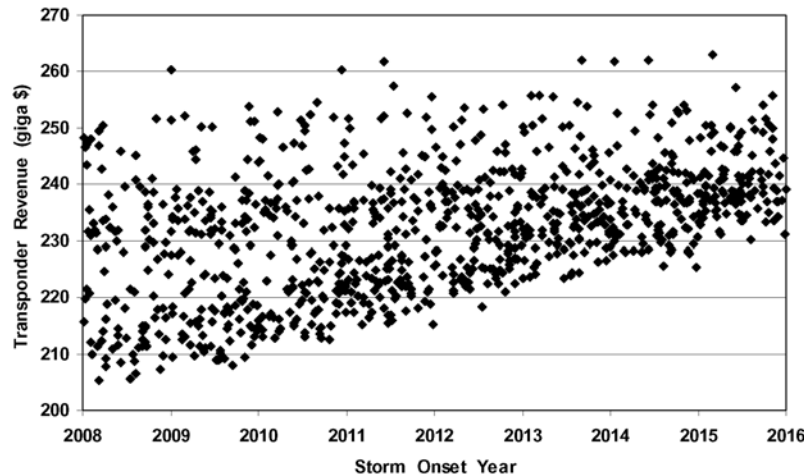


Figure 12. Cumulative transponder revenue versus storm onset year. The vertical dispersion is due to the variation of the storm strength from 200,000 pfu (lower envelope) to 50,000 pfu (upper envelope).

[62] 2. There is considerable uncertainty in forecasting the growth rates for transponder leasing 2–10 years into the future. We made no attempt to determine for each satellite the actual number of leased transponders or the current growth rates.

[63] 3. Insurance payouts, launch costs, asset amortization, and leasing rates dependent upon supply and demand considerations are all factors that significantly alter the calculation of the economic model of superstorm impacts. These can cause the actual profit derived from the ensemble of satellites to vary considerably depending on the exact assumptions made in defining these economic factors. A thorough, and deep, understanding of the economics of the GEO satellite industry is required to sort out this complex financial maze.

[64] 4. No accounting is made for collateral economic losses incurred by transponder subscribers. One transponder can service millions of customers or hundreds of millions of very small aperture terminals used in banking or point-of-sale transactions. When these resources fail for even a few hours, considerable economic disruption can result (e.g., ~30 million lost pagers when Galaxy IV failed in 1998 according to CNN (Pager messages lost in space, 20 May 1998, available at <http://www.cnn.com/TECH/space/9805/20/satellite.outage/>)).

[65] In our next series of models, we will attempt to address some of these issues in what we hope will be progressively more comprehensive models.

[66] **Acknowledgments.** We would like to thank the three referees who reviewed this paper and provided many helpful comments that have, largely, helped us to see these results from very different perspectives. Although we initially attempted to discuss our models from the profit side of the

economic ledger, we now understand more thoroughly than before that no one has an unambiguous definition of this parameter. Consequently, we were saved the embarrassment by our referees of publicly wading into this economic quagmire and were urged to focus instead on a smaller set of parameters and relationships that are likely to be much better defined for satellites.

## References

- Allen, J., and D. Wilkinson (Eds.) (1993), *Solar-Terrestrial Predictions—IV: Proceedings of a Workshop held May 18–22, 1992, at Ottawa, Canada*, vol. 1, *Geomagnetic Papers, Ionospheric Papers*, 75 pp., Environ. Res. Lab., NOAA, Boulder, Colo.
- Brekke, P. (2004), Space weather effects on SOHO and its space weather warning capabilities, in *Effects of Space Weather on Technology Infrastructure*, edited by I. Daglis, pp. 109–122, Kluwer Acad., Boston, Mass.
- Chetty, P. R. K. (1991), *Satellite Technology and its Applications*, 2nd ed., pp. 164–166, McGraw-Hill, New York.
- Cliver, E. W., and L. Svalgaard (2005), The 1859 solar-terrestrial disturbance and the current limits of extreme space weather activity, *Sol. Phys.*, 224, 407–422.
- Commercial Space Transportation Advisory Committee (COMSTAC) (2004), NGSO commercial space transportation forecasts, May 2004, Fed. Aviation Admin., U.S. Dep. of Transp., Washington, D. C.
- Commercial Space Transportation Advisory Committee (COMSTAC) (2005), NGSO Commercial space transportation forecasts, May 2005, Fed. Aviation Admin., U.S. Dep. of Transp., Washington, D. C.
- Crabb, R. L. (1994), Solar cell radiation damage, *Radiat. Phys. Chem.*, 43, 93–103.
- Dikpati, M., G. de Toma, and P. A. Gilman (2006), Predicting the strength of solar cycle 24 using a flux-transport dynamo-based tool, *Geophys. Res. Lett.*, 33, L05102, doi:10.1029/2005GL025221.
- Green, J. L., S. A. Boardsen, S. Odenwald, J. E. Humble, and K. A. Pazamickas (2006), Eyewitness reports of the great auroral storm of 1859, *Adv. Space Res.*, 38, 145–154, doi:10.1016/j.asr.2005.08.0542005.
- Landis, G. A., and L. H. Westerlund (1992), Laser beamed power: Satellite demonstration applications, *NASA Contractor Rep. NASA-CR190793*.

- McCracken, K. G., G. A. M. Dreschhoff, E. J. Zeller, D. F. Smart, and M. A. Shea (2001), Solar cosmic ray events for the period 1561–1994: 1. Identification in polar ice, 1561–1950, *J. Geophys. Res.*, **106**(A10), 21,585–21,598.
- Northern Sky Research (2005), Global assessment of satellite demand, 2nd e., Cambridge, Mass.
- Odenwald, S. F., J. L. Green, and W. W. L. Taylor (2006), Forecasting the impact of an 1859-calibre superstorm on satellite resources, *Adv. Space Res.*, **38**, 280–297, doi:10.1016/j.asr.2005.10.046.
- Patel, M. R. (2000), *Spacecraft Power Systems*, 115 pp., CRC Press, New York.
- Reedy, R. (2002), Recent solar energetic particles: Updates and trends, *Lunar Planet. Sci.*, **XXXIII**, abstract 1938.
- Simonin, B. (2005), SOHO monthly trending report, *SOHO/PRG/TR/613*, Eur. Space Agency, Paris. (Available at [http://sohowww.nascom.nasa.gov/operations/trending/trend\\_200507.pdf](http://sohowww.nascom.nasa.gov/operations/trending/trend_200507.pdf).)
- Smart, M. A., and D. F. Shea (1990), A summary of major solar proton events, *Sol. Phys.*, **127**, 297–320.
- Stephens, D. L., L. W. Townsend, and J. L. Hoff (2005), Interplanetary crew dose estimates for worse-case solar particle events based on historical data for the Carrington flare of 1859, *Acta Astron.*, **56**, 969–974.
- Tada, H. Y., J. R. Carter, B. E. Anspaugh, and R. G. Downing (1982), Solar cell radiation handbook, *JPL Publ. 82-69*, 3rd ed., Jet Propul. Lab., Pasadena, Calif.
- Townsend, L. W. (2003), Carrington flare of 1859 as a prototypical worst-case solar energetic particle event, *IEEE Trans. Nucl. Sci.*, **50**, 2307–2309.
- Tsurutani, B. T., W. D. Gonzalez, G. S. Lakhina, and S. Alex (2003), The extreme magnetic storm of 1–2 September 1859, *J. Geophys. Res.*, **108**(A7), 1268, doi:10.1029/2002JA009504.
- Wiedenbeck, M. E., et al. (2005), The level of solar modulation of galactic cosmic rays from 1997 to 2005 as derived from ACE measurements of elemental energy spectra, paper presented at 29th International Cosmic Ray Conference, Tata Inst. of Fundam. Res., Pune, India, 3–10 Aug.
- 
- J. L. Green and S. F. Odenwald, NASA Goddard Space Flight Center, Greenbelt, MD 20771, USA. (odenwald@astronomycafe.net)